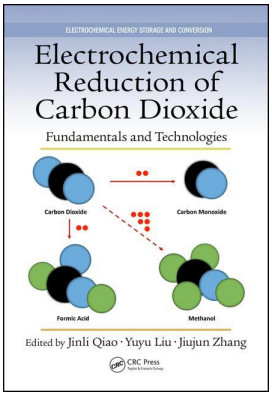

Electrochemical Reduction of Carbon Dioxide Fundamentals and Technologies

Jinli Qiao, Yuyu Liu, Jiujun Zhang

Product Analysis for CO Electroreduction

Publication details
https://test.routledgehandbooks.com/doi/10.1201/b20177-8
Jinli Qiao, Yuyu Liu, Jiujun Zhang
Published online on: 14 Jun 2016

7 Product Analysis for CO_2 Electroreduction

Jingyu Tang, Xiaozhou Zou, and Feng Hong

CONTENTS

7.1 INTRODUCTION

CO_2 electroreduction involves multielectron processes which can form a large variety of products ranging from CO, CH_4 to higher hydrocarbons in the gas phase, and generate various oxygenates in the liquid phase such as alcohols, aldehydes, and carboxylic acids. Currently, controlling the CO_2 reduction pathways is still a challenging work. A thorough and accurate determination of products is of critical importance for the evaluation of electroreduction performance. Many groups have practically adopted the routine analysis of one or two products in either gas or liquid phase for evaluation of electrocatalytic efficiencies. However, to date, only very few studies have been focused on the analysis of reduction products, and more comprehensive and standard analysis methods are not yet reported in the literature. In this chapter, different analysis methods reported so far are summarized.

7.2 SAMPLE PREPARATION

The products of CO_2 electroreduction are affected by the electrode types, composition of electrolyte (aqueous or nonaqueous), and the overpotential. For example, in

aqueous supporting electrolytes, metallic In, Sn, Hg, and Pb are selective for the production of formic acid; metallic Zn, Au, and Ag produce carbon monoxide; metallic Cu exhibits a high electrocatalytic activity for the formation of hydrocarbons, aldehydes, and alcohols, whereas metallic Al, Ga show low electrocatalytic activity in CO_2 electroreduction [1]. In nonaqueous supporting electrolytes on Pb, Tl, and Hg, the main product is oxalic acid; on Cu, Ag, Au, In, Zn, and Sn, carbon monoxide and carbonate ions are obtained, whereas Ni, Pd, and Pt are selective for CO formation; and Al, Ga form both CO and oxalic acid. This information will be very helpful for the product analysis for CO_2 electroreduction.

The products of CO_2 electroreduction can be divided into gas phase and liquid phase. The main products of the electroreduction of carbon dioxide are CH_3CH_3, CO, CH_4, H_2, O_2 in the gas phase, and oxygenates in the liquid phase such as alcohols, aldehydes, and carboxylic acids [2]. So the basic sample preparation is to collect the gas and the liquid products. Then, the next preparation step will be determined by the following analytic methods. For example, when the gas samples are analyzed by gas chromatography (GC) with flame ionization detector (FID), O_2 is usually needed to be removed.

7.3 CHEMICAL ANALYSIS

Many of the products in the liquid phase can be analyzed by chemical methods such as titration. Carbonate/bicarbonate concentration at the cathode side is usually determined by the sequential titration of the catholyte samples with hydrochloric acid, using phenolphthalein and methyl orange as indicators [3]. Carbonate is a stronger base than bicarbonate. At the beginning of titration, with phenolphthalein as the indicator, only carbonate reacts with hydrochloric forming bicarbonate. The red color of phenolphthalein will disappear when all carbonate turns into bicarbonate. The concentration of carbonate can be calculated according to the volume and concentration of the hydrochloric acid. Then methyl orange is added to the solution as an indicator for the titration of bicarbonate. The yellow solution turns into orange when the titration is just finished. The bicarbonate quantity obtained from the titration calculation consists of the original bicarbonate in the sample and the bicarbonate transformed from the titration of carbonate. As the quantity of carbonate has been estimated in the first step of titration, the bicarbonate concentration in the sample can be deduced sequentially.

Methanol/formaldehyde can be estimated by back titration with ferrous ammonium sulfate of the product from acid dichromate oxidation [2]. An alkaline permanganate oxidation technique can be used to quantify the formate in the cathodic liquid products [3]. Before titration, formic acid and formate are treated with an excess of sodium carbonate. The standard potassium permanganate solution is added to the hot formate solution until the clear liquid above the precipitate is just colored pink. In order to detect the exact end point in the presence of the brown precipitate, the pink solution is strongly acidified with dilute sulfuric acid, and also a known excess 0.1 N sodium oxalate solution is added, then the mixture is warmed until the precipitate has dissolved. The excess of oxalate is titrated with standard potassium

permanganate solution. The quantity of formic acid and formate is calculated by using the conversion formula: 1 mL of 1 N $KMnO_4$ = 0.02301 g HCOOH.

7.4 INSTRUMENTAL ANALYSIS

7.4.1 Gas Chromatography

GC is the most commonly used method for quantification of the gas species [4–9]. When the gas flows into the column, the column packing may adsorb CH_3CH_3, CO, CH_4, H_2, and other components differently, which cause different flow rates of different compounds under the impetus of the mobile phase. Then the compounds will be separated and detected when they get out of the column. The elution order and retention time are the main data for the identification of the products. The amount of the compounds can be calculated from the integral area of the chromatography peaks. It is reported that many types of column have been used for the separation of the CO_2 electroreduction products, such as carbon columns [10–13], molecular sieves [7,14], and Poraplot Q [6,8,9,15,16]. Thermal conductivity detector (TCD) and FID are the most commonly used detectors in GC. Both are sensitive for many compounds. FID is more sensitive than TCD for the analysis of low concentrations of CO and hydrocarbons. FID analysis is a destructive method. Therefore, the gas should first be analyzed by TCD for gas quantification followed by FID for the analysis of CO and alkanes [4]. GC calibration lines of some common products of CO_2 electroreduction, from which the linear correlativity between the peak area and the compound concentration can be used to quantify the products, always indicates high degree of accuracy of GC with a correlation index R^2 of almost close to 1.

However, the presence of CO_2 in the product stream can cause deactivation of certain types of columns, including the most commonly used molecular sieve column. Hong et al. [4] designed a better GC configuration to separate and detect all the gases, including CH_4, CH_3CH_3, CO, CO_2, O_2, N_2, and H_2 for product analysis of photocatalytic reduction of CO_2. The GC configuration can avoid regular column regeneration and achieve longer lifetime of the detector. Figure 7.1 shows the simplified configuration of their GC. Helium (99.9995%) was used as the carrier gas. The back channel of GC is equipped with two packed columns, Hayesep Q and Molsieve 5 Å, and three gas switch valves, V1–V3. During the analysis, 0.25 mL of gas sample in the sample loop of V1 was introduced to the Hayesep Q column where CO_2 was separated from the other gases due to its longer retention time. The other gases can be completely eluted from the first column and enter the Molsieve column before 2.5 min. At 2.5 min, Valve 2 is switched for CO_2 to bypass the Molsieve column and be detected by TCD. After TCD analysis, CO_2 is vented out by the switch of Valve 3 during 3–7 min. The rest of the gases after the Hayesep Q column were further separated by the Molsieve 5 Å column. At 10 min, V2 is switched back for these separated gases to be detected by TCD and then CH_4, CO, and CH_3CH_3 were further detected by FID with higher sensitivities. The role of the methanizer (nickel catalyst) is to convert CO to CH_4 for FID analysis, whereas alkanes remained unaffected. During this process, the GC oven was held at 60°C for 15 min and increased to 180°C for 5 min for the postrun.

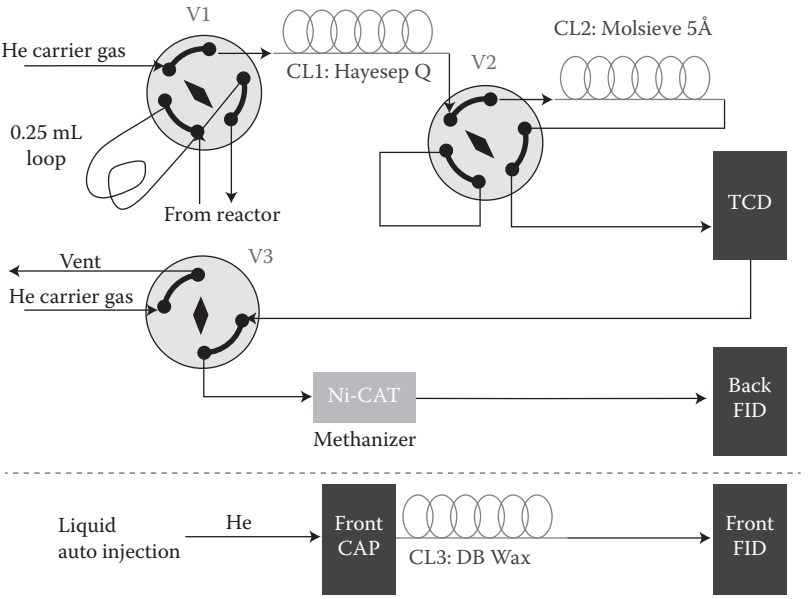

FIGURE 7.1 Flowchart of gas chromatography for gas-phase product analysis and liquid-phase analysis of alcohols. V1–V3: gas switch valves, CL1–3: separation columns. (Reprinted by permission from Hong, J., Zhang, W., Ren, J., Xu, R., *Anal. Methods*, 5 (5), 1086–1097, 2013.)

GC with TCD/FID is also the main technique used for the analysis of different types of liquid oxygenates (mainly alcohols) [7–9,14,17]. Alcohols in the liquid phase are volatile compounds and can be easily vaporized into gases during the vaporization process. Then, gases such as CH_4, CH_3CH_3, CO, CO_2, O_2, N_2 described above will be separated and tested. For example, methanol can be analyzed by GC equipped with a DB-Wax column and a FID detector [18]. However, alcohol analysis is very sensitive to the alkaline conditions and organics in terms of peak areas [4]. Figure 7.2 illustrates the effect of organics and alkaline conditions to methanol, ethanol, and 1-propanol analysis.

However, carbonate, bicarbonate, and other salt compounds in the liquid sample are not easy to vaporize or easy to decompose when heated. GC is not suitable for the analysis of these compounds. Other methods such as high-performance liquid chromatography (HPLC), ion exchange chromatography (IEC), ultraviolet (UV)–visible spectroscopy (colorimetric assay), and nuclear magnetic resonance (NMR) are used to analyze the compounds in the liquid-phase products.

7.4.2 Mass Spectrometry

Mass spectrometry (MS) is often equipped with GC to identify the compounds in the sample for its unique identification capability and high sensitivity [19–23]. During the GC–MS analysis, compounds are first separated by the GC column, and then the eluates are injected into MS for further analysis. Usually, nuclear mass ratio is the

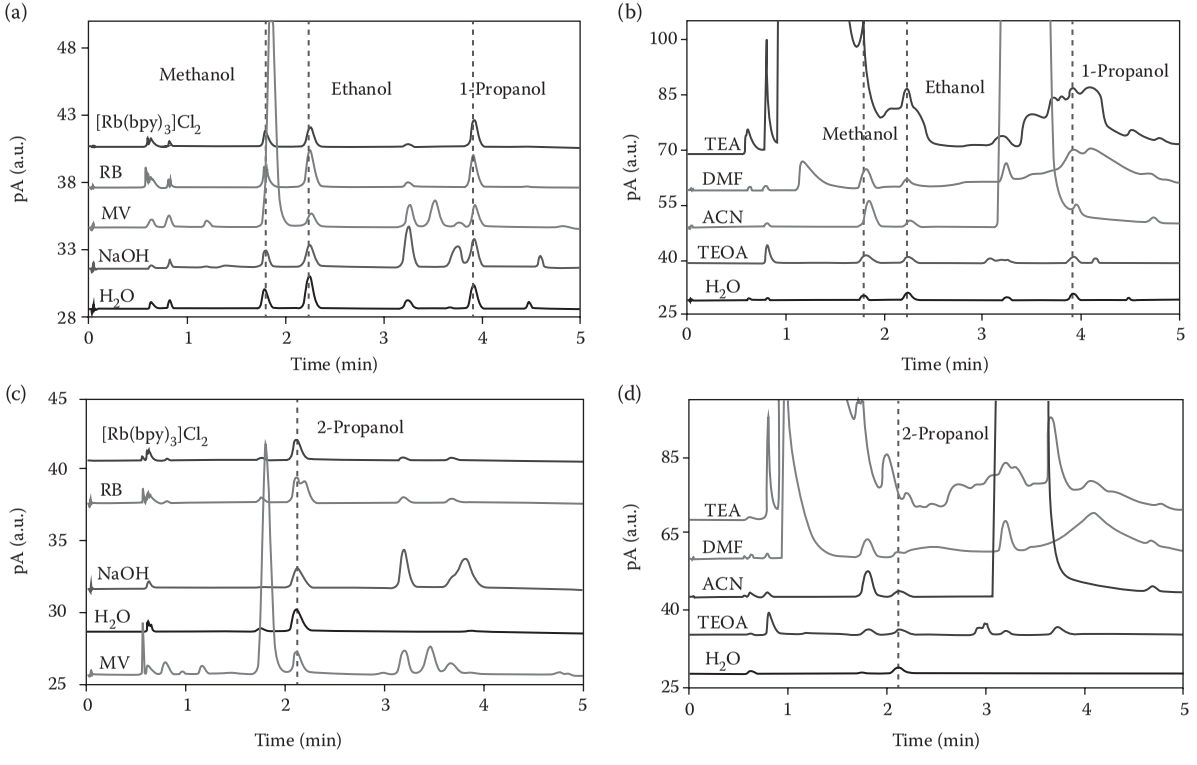

FIGURE 7.2 GC peaks of methanol, ethanol, 1-propanol in (a) 0.1 M NaOH, 0.1 mM methyl viologen (MV), 0.1 mM rose bengal (RB), 0.1 mM $[Ru(bpy)_3]Cl_2$, and (b) 15 v% acetonitrile (ACN), 15 v% dimethylformamide (DMF), 15 v% triethylamine (TEA), 15 v% triethanolamine (TEOA); GC peaks of 2-propanol in (c) 0.1 M NaOH, 0.1 mM MV, 0.1 mM RB, 0.1 mM $[Ru(bpy)_3]Cl_2$; and (d) 15 v% ACN, 15 v% DMF, 15 v% TEA, 15 v% TEOA. (Reprinted by permission from Hong, J., Zhang, W., Ren, J., Xu, R., *Anal. Methods*, 5(5), 1086–1097, 2013.)

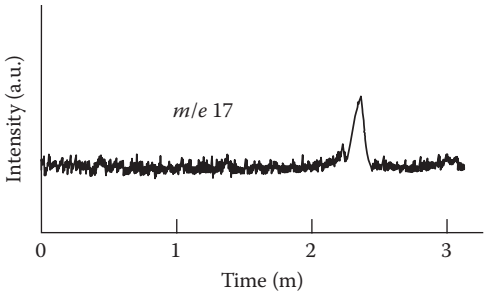

FIGURE 7.3 GC–MS chromatogram at $m/e = 17$ attributable to $^{13}CH_4$ of the gas sample produced by the photocatalytic reaction using Pd (2%)-TiO_2 under a $^{13}CO_2$ atmosphere. (Reprinted by permission from Yui, T., Kan, A., Saitoh, C., Koike, K., Ibusuki, T., Ishitani, O., *ACS Appl. Mater. Interfaces*, 3 (7), 2594–2600, 2011.)

main data from the MS analysis. As the main products in electroreduction of CO_2 are some simple compounds such as CH_4, CH_3CH_3, CO, alcohols, aldehydes, and carboxylic acids, the nuclear mass data will be very helpful to identify the components of the products. For example, the $m/e = 17$ signal in a GC–MS chromatogram of the gas sample shown in Figure 7.3 is attributed to $^{13}CH_4$.

7.4.3 Infrared Spectroscopy

Infrared spectroscopy (IR) or diffuse reflectance infrared Fourier transform spectroscopy (DRIFT) has occasionally been employed to verify the consumption of CO_2 and the generation of CO [25–27]. IR or DRIFT analysis can give the functional group composition of the compounds separated by GC. Then the compounds separated by GC can be easily identified by the obtained IR/DRIFT data and the MS data. However, MS and IR/DRIFT are not suitable for the quantitative analysis of the components in the products of CO_2 electroreduction [4]. Figure 7.4 shows the *in situ* Fourier transform infrared spectroscopy (FT-IR) spectra using p-polarized light. Spectra were recorded at controlled potential for electrolyte solution saturated with CO_2 (Figure 7.4a) and in the absence of CO_2 (Figure 7.4b). Only the region between 1150 and 2000 cm^{-1} is shown and remarkable differences are observed in this region. For the DMF solution saturated with CO_2 (Figure 7.4a), the most interesting features, with loss (i) and gain (ii) of absorbance, are: (i) 1759, 1670, 1508, 1410, 1262 cm^{-1}; (ii) 1732, 1639, 1604, 1478, 1370, 1330, 1300 cm^{-1}, and for the CO_2-free solution (Figure 7.4b): (i) 1662, 1508, 1473, 1406, 1391, 1362, 1223 cm^{-1}; (ii) 1739, 1566, and 1473 cm^{-1} [28].

7.4.4 Nuclear Magnetic Resonance

NMR is also used to qualify the compounds in the sample [29,30]. It is usually equipped with GC or GC–MS. Almost all oxygenates in the products can be identified by this method. The compounds in the sample are first separated and then quantified by GC. MS is used to detect the molecular weight of the separated compounds.

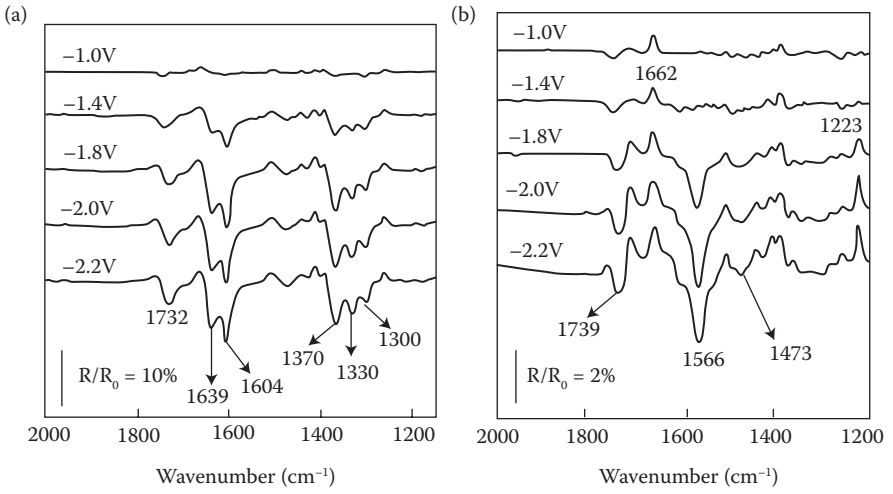

FIGURE 7.4 *In situ* FT-IR external reflectance spectra on smooth gold with modulated potential. (IR region 1150–2000 cm^{-1}). P-polarized light. (a) DMF + TBAF (TBAF; 0.15 mol/dm^3) saturated with CO_2 and (b) without CO_2. Potentials vs. SCE. Temperature: 20°C. (Reprinted by permission from Pérez, E.R., Garcia, J.R., Cardoso, D.R., McGarvey, B.R., Batista, E.A., Rodrigues-Filho, U.P., Vielstich, W., Franco, D.W., *J. Electroanal. Chem.*, 578 (1), 87–94, 2005.)

^1H or ^{13}C NMR analysis is then taken for structure analysis. Figure 7.5 shows ^1H NMR spectra of formate produced from CO_2 reduction, from which ^1H NMR signal of some compounds such as formate and water can be identified easily. Also like IR and MS, NMR is difficult for the quantification of the compounds. However, some work demonstrated the quantification of the products by NMR [31]. Formate products in aqueous solution were reported to be quantified by NMR with sodium 3-(trimethylsilyl) propionate 2,2,3,3-d (TSP) as an internal standard [30]. The chemical shift of the hydrogen atom in the CH group in formate ($HCOO^-$) is at about 8.443 ppm, whereas 0 ppm is assigned to the resonance of the CH_3 group of TSP. Formate concentration was determined with reference to the peak area of the CH proton in formate to that of the CH_3 protons in TSP. A calibration curve can be made by plotting the concentrations of standard formic acid solutions versus the concentrations measured by NMR. The formate concentration is then obtained by fitting the calibration curve. Figure 7.6 illustrates ^1H NMR spectra of formate and CH_3 and CH_2 groups produced from CO_2 reduction at controlled potential, which will contribute to identify the components of the products for CO_2 electroreduction. ^{13}C NMR also can be used to verify the origination of the products in the sample of CO_2 electroreduction. The disadvantage for the use of NMR is its high cost.

7.4.5 Spectrophotometric Method

UV and visible spectrophotometry is widely used to quantify many compounds. Products such as formaldehyde and formate can be detected and quantified through

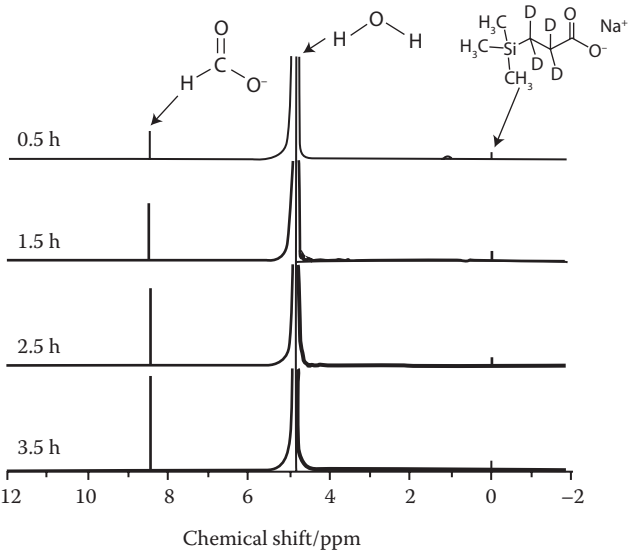

FIGURE 7.5 ^{1}H NMR spectra of formate produced from CO_2 reduction at $E = -2$ V vs. SCE in 0.5 M $KHCO_3$. (Reprinted by permission from Wu, J., Risalvato, F.G., Ke, F.-S., Pellechia, P., Zhou, X.-D., *J. Electroanal. Chem.*, 159 (7), F353–F359, 2012. The Electrochemical Society.)

the chromotropic acid test, which is a spectrophotometric method [33]. For the determination of formaldehyde, the sample is usually first diluted with sulfuric acid properly. Chromotropic acid is subsequently added and the solution is heated in a water bath at 60°C for 30 min. The absorbance of the solution at 484 and 578 nm is obtained and compared with those values obtained from a calibration curve using standard formaldehyde solutions. For the determination of formate, the electrolyzed solution is initially reduced with Mg/HCl and the same procedure is subsequently followed as described above. The amount of formate is determined by comparison of difference.

Formate production also can be measured by using UV–Visible spectrophotometry with the broad absorption region of 190–250 nm, as shown in Figure 7.7 [34]. Product samples are first acidified with sulfuric acid to neutralize bicarbonates/hydroxide/carbonates, and then boiled for 10 min to expel carbon dioxide from the solutions. The reference cell in the spectrophotometer is also filled with an appropriate concentration of sulfate as same as in the sample cell. The absorption at 230 nm is chosen for the formate concentration determination because of the saturation of the peak at 208 nm. The formate concentration is finally obtained from a calibration curve of standard formate solutions. The boiling step in this method is important because the UV absorption peaks for carbonates and carbon dioxide interfere with that of formate. With this method, cumulative efficiency of formate production at 40 Ma/cm^2 in a Nafion membrane cell with various cathode solutions was compared, as shown in Figure 7.8 [34].

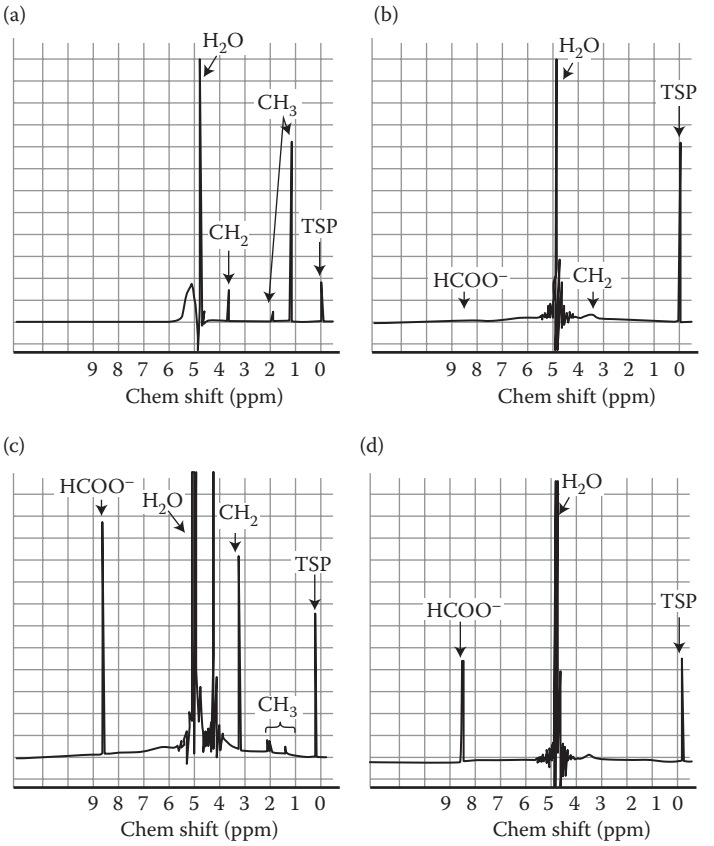

FIGURE 7.6 ^1H NMR spectra of formate and CH_3 and CH_2 groups produced from CO_2 reduction at controlled potential; (a) and (b): $E = -0.8$ and -1.1 V vs. Ag/AgCl in 0.5 M $KHCO_3$ for 90 min, Cu electrode surface obtained by pre-electroreduction in 1 M NaOH at -3.0 V for 10 min; (c) $E = -1.1$ V vs. Ag/AgCl in 0.5 M $KHCO_3$ for 90 min, Cu electrode surface obtained by pre-electroreduction in 1 M H_3PO_4 at -3.0 V for 10 min; (d) the standard ^1H NMR spectra of HCOOH. (Reprinted by permission from Qiao, J., Jiang, P., Liu, J., Zhang, J., *Electrochem. Commun.*, 38, 8–11, 2014.)

7.4.6 High-Performance Liquid Chromatography

HPLC is a technique used to separate, identify, and quantify components in a mixture. This analytical method relies on a column filled with a solid adsorbent material, a mobile phase containing the sample mixture to reach the purpose of component separation. Pumps are used to pass the pressurized liquid mobile phase through columns. The components in the mixture interact differently with the adsorbent materials in the columns, leading to different flow rates for the various components. In the end, the components flow out from the column in order and can be detected by different detectors. The detectors must ensure the components from samples to give signals, which can be used for further analyses. Here, two typical types of detectors

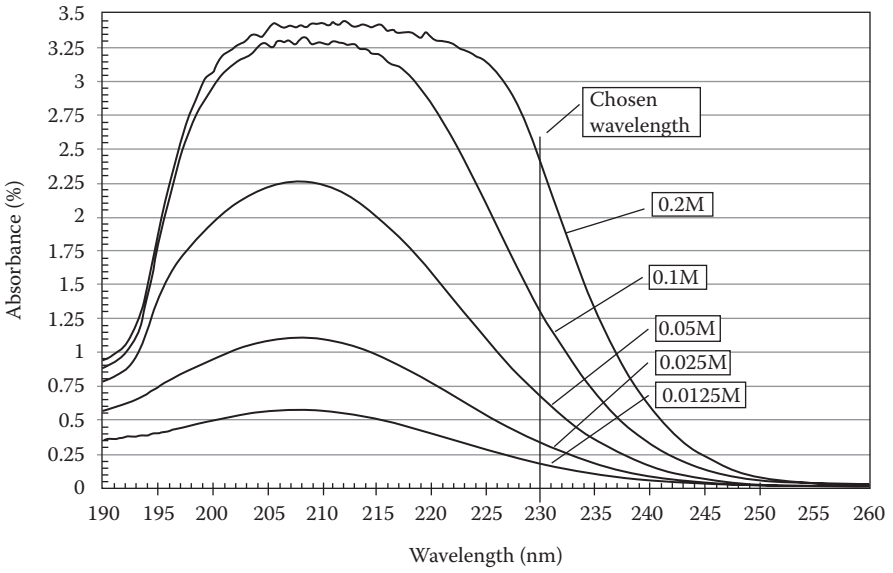

FIGURE 7.7 UV–visible spectra for various concentrations of solutions of sodium formate acidified with sulfuric acid. (Reprinted by permission from Narayanan, S., Haines, B., Soler, J., Valdez, T., *J. Electroanal. Chem.*, 158 (2), A167–A173, 2011. The Electrochemical Society.)

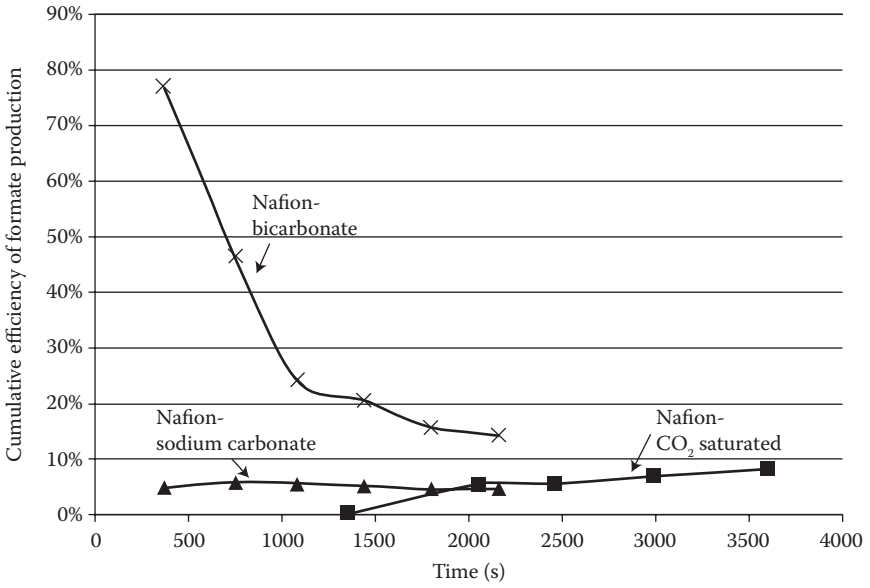

FIGURE 7.8 Cumulative efficiency of formate production at 40 Ma/cm^2 in a Nafion membrane cell with various cathode solutions as indicated. (Reprinted by permission from Narayanan, S., Haines, B., Soler, J., Valdez, T., *J. Electroanal. Chem.*, 158 (2), A167–A173, 2011. The Electrochemical Society.)

are introduced as examples, the diode array detector (DAD) and reflective index detector (RID). A DAD is usually used to detect products based on their absorption of UV/visible light. A DAD detector provides multiple photodiode arrays that enable the detector to obtain information from a wide range of wave lengths. An RID works on the basis of the difference of refraction index between components from the sample and the mobile phase. Different products have different retention time, and the shift of product peak to a different retention time in HPLC always signifies different products. Both qualitative and quantitative information of the components can be received with the help of the obtained graphs.

HPLC has been used frequently to determine the liquid-phase products in the reactions of electrochemical reduction of carbon dioxide. HPLC allows separation of the compounds of the reaction mixture using different interactions with a liquid mobile phase and a solid stationary phase. For the analysis of the products, only a small volume of the sample is needed to be mixed with a solvent. The mixture is then forced to pass through the column under a high pressure which is given by pumps. The different components in the mixture move through the column with different rates, which depend on their own characteristics. Components such as formic acid, oxalic acid, and formaldehyde are often analyzed by HPLC [18,35–40]. Similarly with GC, the identification and quantization of the products by using HPLC also need calibration lines of standard compounds. Various organics and alkaline conditions may affect the acid analysis. Figure 7.9 illustrates HPLC peaks of formic acid and acetic acid obtained with different conditions.

Formic acid has been analyzed by using the following columns: Aminex ion exclusion column type HPX-87X [35], Shodex Ionpack KC-811 column [36,37], ODS-18 column [38,39], Atlantis dC18 column [39], and SupelcoGel C-610H column [40]. HPLC used for detection of formic acid is usually equipped with a UV detector [18,35,37]. For example, an Applied Chromatography Systems HPLC monitor fitted with a 254 nm filter [35] and a UV detector set at 220 nm [36,37] were used. The mobile phase should be chosen depending on the types of column used, for example, 0.0025 M sulfuric acid for an Aminex ion exclusion column type HPX-87X [35], 20% ACN in Milli-Q water as a solvent for Atlantis dC18 column [39].

Together with formic acid, oxalic acid can be analyzed at the same time, for example, an HPLC equipped with a Luna 5-μm C18 column and a UV detector operating at 208 nm, and eluted with 5% H_3PO_4 [41]. Formaldehyde is also analyzed by HPLC, and there can be a modification step before detection [18,42]. The liquid samples containing formaldehyde can be derived with 2,4-dinitrophenylhydrazine (DPNH) to form formaldehyde–DNPH samples, which can be measured by HPLC. An HPLC system was operated with Varian Inertsil 5-μ ODS-2 column (150×4.6 mm) and a UV detector.

7.4.7 Ion Chromatography

Ion chromatography (or IEC) separates ions and polar molecules based on their affinity to different types of ion exchanger. This method can be used for almost all kinds of charged molecules. The products of CO_2 electroreduction, for example, formic acid, formate, and oxalate, can also be detected with this method.

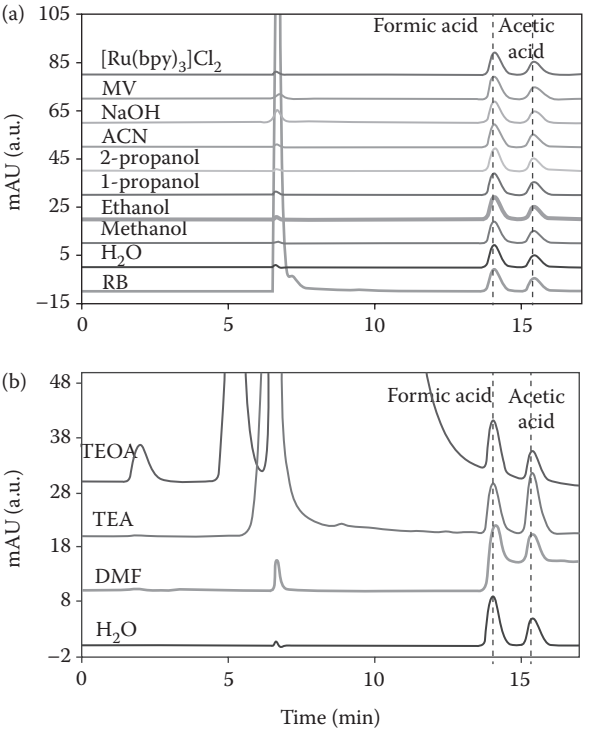

FIGURE 7.9 HPLC peaks of formic acid and acetic acid in (a) 15 v% methanol, 15 v% ethanol, 15 v% 1-propanol, 15 v% 2-propanol, 15 v% ACN, 0.1 M NaOH, 0.1 mM MV, 0.1 mM [Ru(bpy)3]Cl_2, and 0.1 mM RB, and (b) 15 v% DMF, 15 v% TEA, and 15 v% TEOA. (Reprinted by permission from Hong, J., Zhang, W., Ren, J., Xu, R., *Anal. Methods*, 5 (5), 1086–1097, 2013.)

Formic acid in liquid samples was analyzed by this method with, for example, an IonPac AC20 column (4 × 250 mm) equipped with an ED40 conductance detector. There are other cases of formic acid analysis by ion chromatography ICS-900 Dionex using an AS23 analytical column and Na_2CO_3/$NaHCO_3$ as mobile phase [42–44].

Formate ion can be analyzed by the IC [45–47]. The ion exclusion chromatography system can be equipped with, for example, a Dionex AS15 column (2250 mm), an IonPac AG15 guard column (250 mm), and suppressed conductivity ICS-2000 detector [46]. Oxalate can be analyzed by the IC equipped with a UV detector operating at 210 nm and an Aminex HPX-87H ion exchange column eluted with 0.005 mol/dm^3 H_2SO_4, on which conversion of oxalate to oxalic acid takes place [48]. However, this system using Aminex HPX-87H and UV detector is often classified to HPLC.

7.5 ELECTROCHEMICAL ANALYSIS

Reaction rates for the processes of the reduction of carbon dioxide to liquid fuels, which is accomplished through photovoltaic or other electrochemical ways, can be

estimated from the steady-state limiting current in cyclic voltammetry or by rotating disk voltammetry studies [49].

7.5.1 Cyclic Voltammetry

Cyclic voltammetry is the most popular nondestructive technique applied to homogeneous catalysis systems [50]. It is widely used for first evaluation of the catalyst to determine potential of the catalytic process and the catalytic efficiency. Cyclic voltammetry consists of sweeping the potential back and forward at a fixed scan rate (dE/dt) while recording the current response. The obtained curve is known as cyclic voltammogram (CV), and its shape depends on the processes occurring at the electrode surfaces.

In a cyclic voltammetry experiment, the working electrode potential is ramped linearly versus time. During the anodic sweep toward positive potentials, oxidation processes are observed as a positive current, whereas in the cathodic sweep toward negative potentials, the reduction reactions are observed as a negative current. Because these processes are surface sensitive, the shape of the CV gives the information about the structure and the chemical nature of the electrode surface and the composition of the electrolyte. That is why CVs are considered as fingerprints of surfaces. Cyclic voltammetry is further used in a more detailed kinetic analysis to explain the mechanism of the catalytic reaction, and thus to be used to study electrochemical reactions.

Cyclic voltammetry can provide thermodynamic and kinetic information of the processes occurring at the electrode–electrolyte interface, and thus can also be used to determine CO product in electrochemical reactions. After adsorbing CO onto the surface, the potential can be swept toward positive values, and a positive current is observed due to the oxidation of CO.

7.5.2 Rotating Disk Voltammetry and Rotating-Ring Disk Voltammetry

Rotating disk electrode (RDE) voltammetry is a technique that has been mostly used in immobilized catalyst systems [50]. As shown in Figure 7.10a, the rapid rotation of the disk drives liquid to flow horizontally out and away from the center disk, thus serving as a motivation for replenished liquid to move axially to form an upward flow as shown by the arrows. The idea is to electrochemically generate a reactive species at the disk and then to monitor the species electrochemically as it is swept past the ring by laminar flow. Considerable information can be obtained about a redox system by rotating disk voltammetry. An initial voltammogram will locate redox couples in solution, giving information about redox potentials and reversibility.

A typical RDE and a rotating ring-disk electrode (RRDE) are both shown in Figure 7.10b. Compared with RDE, the disk of RRDE is encircled by a ring, which functions as a second working electrode. The idea is to generate a product or an intermediate at a disk electrode and collect it at a ring electrode that concentrically surrounds the disk. The product or intermediate is generated by fixing the disk potential at an appropriate value and scanning the ring potential so as to obtain

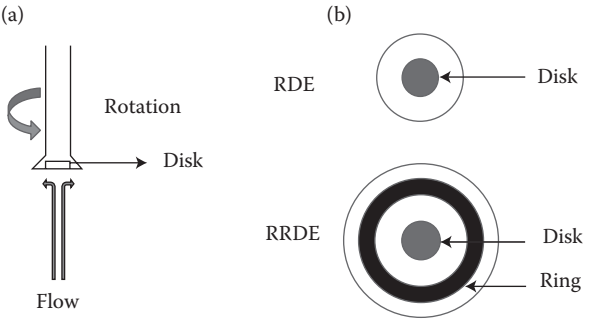

FIGURE 7.10 A typical RDE and a rotating RRDE. (a) RDE with hydrodynamic flow pattern. (b) Bottom view of RDE and RRDE.

its oxidative or reductive signature as a steady-state current–potential curve. This technique is widely used in the study of reaction mechanisms as electroactive intermediates of coupled homogeneous chemical reactions can be monitored at the ring electrode.

RRDE can be used to determine the reduction product of CO_2 both in the liquid phase [51] and in the gas phase [52]. Formic acid can be detected by using the RRDE technique. The formic acid formed on a SnO_2 disk electrode surface as a reduction product of carbon dioxide can be detected at a Pt ring electrode, and its concentration is a parameter for the electrode. With the assumption that HCOOH molecules are all ionized, the detection limit of the present RRDE is expected to be quite close to that value of a pulsed electrochemical detector. Figure 7.11 shows the current–potential curves for a Pt (ring)–Pt (counter) in a 0.1 M Na_2SO_4 solution. Figure 7.12 gives an

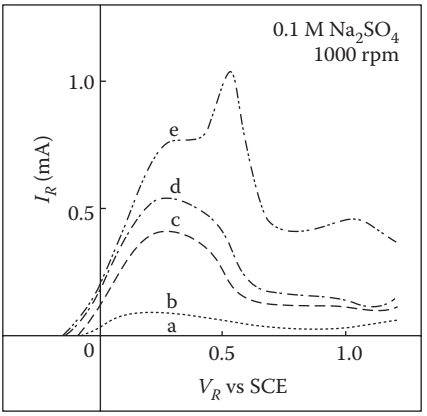

FIGURE 7.11 Current–voltage curves for Pt-ring (anode) with and without HCOOH: (curve a) blank, (curves b–e) with 200, 500, 1000, and 5000 ppm of HCOOH. (Reprinted by permission from Aoki, A., Nogami, G., *J. Electroanal. Chem.*, 142 (2), 423–427, 1995. The Electrochemical Society.)

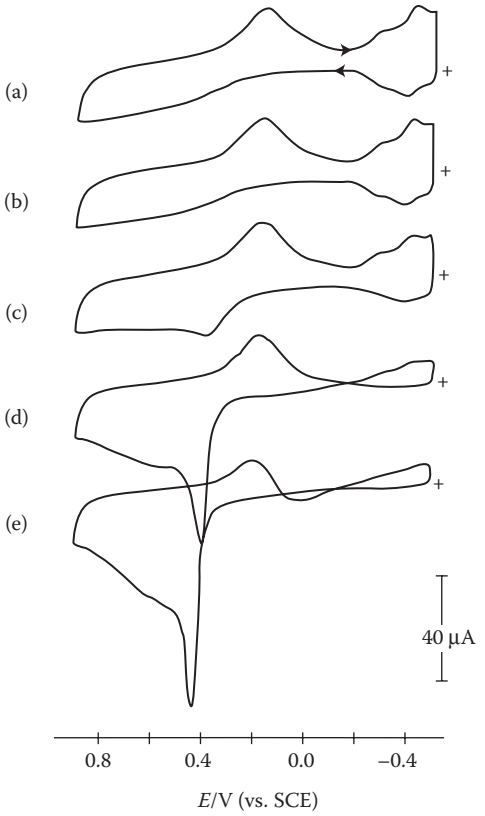

FIGURE 7.12 Ring electrode cyclic votammograms of a rotating ring (platinum)-disk electrode, recorded at different disk electrode potentials: (a) open circuit; (b) –1.0 V; (c) –1.05 V; (d) –1.10 V; and (e) –1.15 V in a 3.2×10^2 M CO_2 solution (pH 5.5). Potential scan rate was 150 mV/s and rotation rate was 900 rpm. (Reprinted by permission from Zhang, J.J., Pietro, W.J., Lever, A.B.P., *J. Electroanal. Chem.*, 403 (1–2), 93–100, 1996.)

example of analysis of CO, which is a main product of CO_2 reduction catalyzed by Co(II) complexes, using the rotating ring (platinum)-disk electrode. The ring potential was scanned continuously in a certain range of voltage in order to define the activity of the platinum ring electrode for CO oxidation. In Figure 7.12a the disk electrode was open circuit and hence no CO is generated. A set of cyclic voltammograms (Figure 7.12b–e) were recorded as the disk electrode potential shifts more negatively into the region where CO_2 is reduced. When the disk electrode was polarized at –1.05 V, a small CO oxidation current near 0.4 V was observed (Figure 7.12c), which indicates that CO is produced at this potential, consistent with the appearance near –1.05 V of the tail where the catalytic current begins to arise in Figure 7.12b. When the potential is polarized more negatively (Figure 7.12d and e), the CO oxidation current grows rapidly, indicating greater production of CO at more negative disk potentials [52].

REFERENCES

1. Jitaru M, Lowy D, Toma M, Toma, B, Oniciu L. Electrochemical reduction of carbon dioxide on flat metallic cathodes. *Journal of Applied Electrochemistry* 1997, 27 (8), 875–889.
2. Li H, Oloman C. The electro-reduction of carbon dioxide in a continuous reactor. *Journal of Applied Electrochemistry* 2005, 35 (10), 955–965.
3. Welcher, F. J. A. Text-book of quantitative inorganic analysis including elementary instrumental analysis (Vogel, Arthur I.). *Journal of Chemical Education* 1963, 40 (1), A68.
4. Hong J, Zhang W, Ren J, Xu R. Photocatalytic reduction of CO_2: A brief review on product analysis and systematic methods. *Analytical Methods* 2013, 5 (5), 1086–1097.
5. Tomita Y, Teruya S, Koga O, Hori Y. Electrochemical reduction of carbon dioxide at a platinum electrode in acetonitrile-water mixtures. *Journal of the Electrochemical Society* 2000, 147 (11), 4164–4167.
6. Azuma M, Hashimoto K, Hiramoto M, Watanabe M, Sakata T. Electrochemical reduction of carbon dioxide on various metal electrodes in low-temperature aqueous $KHCO_3$ media. *Journal of the Electrochemical Society* 1990, 137 (6), 1772–1778.
7. Kaneco S, Iiba K, Katsumata H, Suzuki T, Ohta K. Effect of sodium cation on the electrochemical reduction of CO_2 at a copper electrode in methanol. *Journal of Solid State Electrochemistry* 2007, 11 (4), 490–495.
8. Shiratsuchi R, Nogami G. Pulsed electroreduction of CO_2 on silver electrodes. *Journal of the Electrochemical Society* 1996, 143 (2), 582–586.
9. Aydin R, Köleli F. Electrocatalytic conversion of CO_2 on a polypyrrole electrode under high pressure in methanol. *Synthetic Metals* 2004, 144 (1), 75–80.
10. Wang C, Thompson R. L, Baltrus J, Matranga C. Visible light photoreduction of CO_2 using CdSe/Pt/TiO_2 heterostructured catalysts. *The Journal of Physical Chemistry Letters* 2009, 1 (1), 48–53.
11. Moore G. F, Blakemore J. D, Milot R. L, Hull J. F, Song H.-E, Cai L, Schmuttenmaer C. A, Crabtree R. H, Brudvig G. W. A visible light water-splitting cell with a photoanode formed by codeposition of a high-potential porphyrin and an iridium water-oxidation catalyst. *Energy and Environmental Science* 2011, 4 (7), 2389–2392.
12. Roy L, Zimmerman P. M, Paul A. Changing lanes from concerted to stepwise hydrogenation: The reduction mechanism of frustrated Lewis acid–base pair trapped CO_2 to methanol by ammonia–borane. *Chemistry—A European Journal* 2011, 17 (2), 435–439.
13. Woolerton T. W, Sheard S, Pierce E, Ragsdale S. W, Armstrong F. A. CO_2 photoreduction at enzyme-modified metal oxide nanoparticles. *Energy and Environmental Science* 2011, 4 (7), 2393–2399.
14. Kaneco S, Iiba K, Suzuki S.-k, Ohta K, Mizuno T. Electrochemical reduction of carbon dioxide to hydrocarbons with high Faradaic efficiency in LiOH/methanol. *The Journal of Physical Chemistry B* 1999, 103 (35), 7456–7460.
15. Ohta K, Suda K, Kaneco S, Mizuno T. Electrochemical reduction of carbon dioxide at Cu electrode under ultrasonic irradiation. *Journal of the Electrochemical Society* 2000, 147 (1), 233–237.
16. Magdesieva T, Yamamoto T, Tryk D, Fujishima A. Electrochemical reduction of CO_2 with transition metal phthalocyanine and porphyrin complexes supported on activated carbon fibers. *Journal of the Electrochemical Society* 2002, 149 (6), D89–D95.
17. Kaneco S, Iiba K, Ohta K, Mizuno T. Electrochemical reduction of carbon dioxide on copper in methanol with various potassium supporting electrolytes at low temperature. *Journal of Solid State Electrochemistry* 1999, 3 (7–8), 424–428.
18. Li H, Oloman C. Development of a continuous reactor for the electro-reduction of carbon dioxide to formate—Part 2: Scale-up. *Journal of Applied Electrochemistry* 2007, 37 (10), 1107–1117.

19. Schrebler R, Cury P, Herrera F, Gomez H, Cordova R. Study of the electrochemical reduction of CO_2 on electrodeposited rhenium electrodes in methanol media. *Journal of Electroanalytical Chemistry* 2001, 516 (1), 23–30.
20. Thorson M. R, Siil K. I, Kenis P. J. Effect of cations on the electrochemical conversion of CO_2 to CO. *Journal of the Electrochemical Society* 2013, 160 (1), F69–F74.
21. Hori Y, Takahashi I, Koga O, Hoshi N. Electrochemical reduction of carbon dioxide at various series of copper single crystal electrodes. *Journal of Molecular Catalysis A: Chemical* 2003, 199 (1), 39–47.
22. Yang Z.-Y, Moure V. R, Dean D. R, Seefeldt L. C. Carbon dioxide reduction to methane and coupling with acetylene to form propylene catalyzed by remodeled nitrogenase. *Proceedings of the National Academy of Sciences USA* 2012, 109 (48), 19644–19648.
23. Hori Y, Takahashi I, Koga O, Hoshi N. Selective formation of C2 compounds from electrochemical reduction of CO_2 at a series of copper single crystal electrodes. *The Journal of Physical Chemistry B* 2002, 106 (1), 15–17.
24. Yui T, Kan A, Saitoh C, Koike K, Ibusuki T, Ishitani O. Photochemical reduction of CO_2 using TiO_2: Effects of organic adsorbates on TiO_2 and deposition of Pd onto TiO_2. *ACS Applied Materials & Interfaces* 2011, 3 (7), 2594–2600.
25. Simón-Manso E, Kubiak C. P. Dinuclear nickel complexes as catalysts for electrochemical reduction of carbon dioxide. *Organometallics* 2005, 24 (1), 96–102.
26. Endo N, Miho Y, Ogura K. Hydrogenation of CO_2 on the cathodized tungsten trioxide/polyaniline/polyvinylsulfate-modified electrode in aqueous solution. *Journal of Molecular Catalysis A: Chemical* 1997, 127 (1), 49–56.
27. Schrebler R, Cury P, Suarez C, Munoz E, Gomez H, Cordova R. Study of the electrochemical reduction of CO_2 on a polypyrrole electrode modified by rhenium and copper–rhenium microalloy in methanol media. *Journal of Electroanalytical Chemistry* 2002, 533 (1), 167–175.
28. Pérez E. R, Garcia J. R, Cardoso D. R, McGarvey B. R, Batista E. A, Rodrigues-Filho U. P, Vielstich W, Franco D. W. *In situ* FT-IR and ex situ EPR analysis for the study of the electroreduction of carbon dioxide in *N*,*N*-dimethylformamide on a gold interface. *Journal of Electroanalytical Chemistry* 2005, 578 (1), 87–94.
29. Wang C, Thompson R. L, Ohodnicki P, Baltrus J, Matranga C. Size-dependent photocatalytic reduction of CO_2 with PbS quantum dot sensitized TiO_2 heterostructured photocatalysts. *Journal of Materials Chemistry* 2011, 21 (35), 13452–13457.
30. Wu J, Risalvato F. G, Ke F.-S, Pellechia P, Zhou X.-D. Electrochemical reduction of carbon dioxide I. Effects of the electrolyte on the selectivity and activity with Sn electrode. *Journal of the Electrochemical Society* 2012, 159 (7), F353–F359.
31. Kuhl K. P, Cave E. R, Abram D. N, Jaramillo T. F. New insights into the electrochemical reduction of carbon dioxide on metallic copper surfaces. *Energy and Environmental Science* 2012, 5 (5), 7050–7059.
32. Qiao J, Jiang P, Liu J, Zhang J. Formation of Cu nanostructured electrode surfaces by an annealing–electroreduction procedure to achieve high-efficiency CO_2 electroreduction. *Electrochemistry Communications* 2014, 38, 8–11.
33. Ramos Sende J. A, Arana C. R, Hernandez L, Potts K. T, Keshevarz-K M, Abruna H. D. Electrocatalysis of CO_2 reduction in aqueous media at electrodes modified with electropolymerized films of vinylterpyridine complexes of transition metals. *Inorganic Chemistry* 1995, 34 (12), 3339–3348.
34. Narayanan S, Haines B, Soler J, Valdez T. Electrochemical conversion of carbon dioxide to formate in alkaline polymer electrolyte membrane cells. *Journal of the Electrochemical Society* 2011, 158 (2), A167–A173.
35. Mahmood M. N, Masheder D, Harty C. J. Use of gas-diffusion electrodes for high-rate electrochemical reduction of carbon-dioxide .1. Reduction at lead, indium-impregnated

and tin-impregnated electrodes. *Journal of Applied Electrochemistry* 1987, 17 (6), 1159–1170.
36. Hara K, Kudo A, Sakata T. Electrochemical reduction of carbon-dioxide under high-pressure on various electrodes in an aqueous-electrolyte. *Journal of Electroanalytical Chemistry* 1995, 391 (1–2), 141–147.
37. Sonoyama N, Kirii M, Sakata T. Electrochemical reduction of CO_2 at metal-porphyrin supported gas diffusion electrodes under high pressure CO_2. *Electrochemistry Communications* 1999, 1 (6), 213–216.
38. Koleli F, Balun D. Reduction of CO_2 under high pressure and high temperature on Pb-granule electrodes in a fixed-bed reactor in aqueous medium. *Applied Catalysis A-General* 2004, 274 (1–2), 237–242.
39. Zhang A. J, Zhang W. M, Lu J. X, Wallace G. G, Chen J. Electrocatalytic reduction of carbon dioxide by cobalt-phthalocyanine-incorporated polypyrrole. *Journal of Solid State Electrochemistry* 2009, 12 (8), E17–E19.
40. Prakash G. K. S, Viva F. A, Olah G. A. Electrochemical reduction of CO2 over Sn-Nafion (R) coated electrode for a fuel-cell-like device. *Journal of Power Sources* 2013, 223, 68–73.
41. Manfred Rudolph S. D. Ernst-Gottfried Jager Macrocyclic [$N4^{2-}$] coordinated nickel complexes as catalysts for the formation of oxalate by electrochemical reduction of carbon dioxide. *Journal of American Chemical Society* 2000, 122 (44), 10821–10830.
42. Peng Y. P, Yeh Y. T, Shah S. I, Huang C. P. Concurrent photoelectrochemical reduction of CO_2 and oxidation of methyl orange using nitrogen-doped TiO_2. *Applied Catalysis B-Environment* 2012, 123–124, 414–423.
43. Zhao H. Z, Chang Y. Y, Liu C. Electrodes modified with iron porphyrin and carbon nanotubes: application to CO_2 reduction and mechanism of synergistic electrocatalysis. *Journal of Solid State Electrochemistry* 2013, 17 (6), 1657–1664.
44. Zhao H. Z, Zhang Y, Zhao B, Chang Y. Y, Li Z. S. Electrochemical reduction of carbon dioxide in an MFC-MEC system with a layer-by-layer self-assembly carbon nanotube/cobalt phthalocyanine modified electrode. *Environmental Science and Technology* 2012, 46 (9), 5198–5204.
45. Hori Y, Kikuchi K, Suzuki S. Production of Co and Ch4 in electrochemical reduction of CO_2 at metal-electrodes in aqueous hydrogencarbonate solution. *Chemistry Letters* 1985, 14 (11), 1695–1698.
46. Reda T, Plugge C. M, Abram N. J, Hirst J. Reversible interconversion of carbon dioxide and formate by an electroactive enzyme. *Proceedings of National Academy of Sciences USA* 2008, 105 (31), 10654–10658.
47. Alvarez-Guerra M, Quintanilla S, Irabien A. Conversion of carbon dioxide into formate using a continuous electrochemical reduction process in a lead cathode. *Chemical Engineering Journal* 2012, 207, 278–284.
48. Kudo K, Ikoma F, Mori S, Komatsu K, Sugita N. Novel synthesis of oxalate from carbon-dioxide and carbon-monoxide in the presence of cesium carbonate. *Journal of Chemical Society, Chemical Communications* 1995, (6), 633–634.
49. Benson E. E, Kubiak C. P, Sathrum A. J, Smieja J. M. Electrocatalytic and homogeneous approaches to conversion of CO_2 to liquid fuels. *Chemical Society Review* 2009, 38 (1), 89–99.
50. Saveant J. M. Molecular catalysis of electrochemical reactions. Mechanistic aspects. *Chemical Reviews* 2008, 108 (7), 2348–2378.
51. Aoki A, Nogami G. Rotating ring-disk electrode study on the fixation mechanism of carbon dioxide. *Journal of Electrochemical Society* 1995, 142 (2), 423–427.
52. Zhang J. J, Pietro W. J, Lever A. B. P. Rotating ring-disk electrode analysis of CO_2 reduction electrocatalyzed by a cobalt tetramethylpyridoporphyrazine on the disk and detected as CO on a platinum ring. *Journal of Electroanalytical Chemistry* 1996, 403 (1–2), 93–100.